Statistical Properties of High-Speed Train Wireless Channels in Different Scenarios

Yu Liu[1], Yapei Zhang[1], Ammar Ghazal[2], Cheng-Xiang Wang[1,2], Yang Yang[3]
[1]School of Information Science and Engineering, Shandong University, Jinan, Shandong, China
[2]Institute of Sensors, Signals and Systems, School of EPS, Heriot-Watt University, Edinburgh, EH14 4AS, UK
[3]Shanghai Research Center for Wireless Communications (WiCO), Shanghai, 201210, China
Email: {xinwenliuyu, ypzhangsdu,}@163.com, {ag289, cheng-xiang.wang,}@hw.ac.uk, yang.yang@wico.sh

***Abstract*—In this paper, we compare the statistical properties of high-speed train (HST) wireless channels in different scenarios using a generic non-stationary HST channel model that has been verified by channel measurement [1]. We mainly focus our comparison and analysis on the three most common HST scenarios, i.e., the rural area, cutting, and viaduct scenarios. Several channel statistical properties such as the temporal autocorrelation function (ACF), space cross-correlation function (CCF), and space-Doppler (SD) power spectrum density (PSD) are investigated. The impacts of different scenario-specific parameters on the channel statistical properties are also studied via numerical analysis.**

***Index Terms*—High-speed train wireless channels, HST scenarios, statistical properties.**

I. Introduction

In the modern society, HST as a fast and convenient transportation tool has experienced a rapid development. HST communication systems have also attracted more and more attention recently. With the conventional HST communication network architecture, HST users inside trains directly communicate with outdoor base stations (BSs), which can cause a lot of problems such as large Doppler spread, fast handover, limited visibility in tunnels, and high penetration losses [2]. Also, HST communication systems need to be more reliable and face many challenges resulting from the high moving speed that can easily exceed 250 km/h.

To overcome these problems, some cellular architectures have been proposed for future HST communication systems, such as the mobile relay station (MRS) [3], coordinated multipoint (CoMP) [4], and distributed antenna system (DAS) [3]. Regardless the adopted HST communication systems, accurate channel models which can characterize real HST channel environments are essential. A better understanding of HST channel characteristics is important and necessary [2]. There are many statistical properties that can be used to describe the channel information, including the first order statistics, such as mean, variance, probability density function (PDF), and cumulative distribution function (CDF), and the second order statistics, such as the ACF, space CCF, PSD, level crossing rate (LCR), and average fade duration (AFD). When the train travels on the track, it will encounter more than 12 scenarios, such as rural area, cutting, viaduct, hilly terrain, tunnel, and station scenarios [5]. Different scenarios introduce different scattering environments and will result in different channel characteristics.

In [6], some channel statistical properties in HST cutting scenarios were introduced, such as fade depth (FD), amplitude distribution, LCR, and ACF. The study in [7] presented the analysis of FD, LCR, AFD, and fading distributions in HST viaduct scenarios. Moreover, propagation characteristics including LCR, AFD, and FD for HST station scenarios were presented in [8]. All the previous studies tend to analyze HST channel characteristics in a specific single scenario and did not discuss the difference of the channel statistical properties of different scenarios. To fill this gap, we compare the channel statistical properties and analyze the difference under different HST propagation scenarios.

The rest of this paper is organized as follows. Several common HST scenarios and network architectures are introduced in Section II. In Section III, a geometry-based stochastic model (GBSM) for HSTs is presented and the statistical properties in different HST scenarios are compared. The corresponding numerical and simulation results are given in Section IV. Finally, the conclusions are drawn in Section V.

II. Classical HST scenarios and network architecture

During its travel, a HST can encounter different environments. These environments can be roughly divided into several scenarios, such as rural area, viaduct, cutting, tunnel, and station scenarios. Different scenarios lead to different scattering conditions, which will have a significant impact on the underlying HST propagation characteristics.

A. HST scenarios

1) Rural area scenario: The rural area scenario, as one of the most common HST scenarios, is relatively flat and wide area. In this scenario, the BS antenna is much higher than the surroundings. Therefore, the line-of-sight (LoS) component is normally dominant between the transmitter and the moving receiver. After traveling a certain distance, the impact of the scatterers will begin to appear and gradually increase at the receiver side which will be presented by lots of non-LoS (NLoS) components resulted from such as reflections, scatterings and diffractions phenomena [9].

978-1-5090-1698-3/16/$31.00 ©2016 IEEE

2) Viaduct scenario: Viaduct scenario is also one of the most encountered HST scenarios. Viaduct is usually used to ensure the smoothness of railway and the high speed of a train. It also can be used to reduce the reflections, scattering and diffractions by cutting down the number of scatterings, such as the trees and architectures around the receiver [5]. To achieve this goal, the height of transmitter antennas is usually set as 20-30 m higher than the surface of the railway track. In this scenario, the LoS component is dominant and the sparsity of the scatterers around the viaducts will have minor impact on the received signal [9].

3) Cutting scenario: The cutting scenario, as another common HST scenario, is also widely used for the HST construction to ensure the smoothness of railway track and to help achieving high speed when travel through the hills. Generally, the cutting scenarios can be divided into two types: the regular form with almost the same depths and slopes steep walls on both sides of railway, and irregular one with irregular hills along the track [5], [9]. Here, the scatterers at the receivers are relatively rich, and LoS components can be observed along the travel route.

4) Tunnel scenario: Tunnels are usually used to ensure stable and high speed of train travel among the hills. Due to its unique environment, such as smooth walls and close structure, there are rich scatterers inside tunnel, which bring the waveguide effects. This makes the signal propagation inside tunnel very different from the other HST scenarios [10], [11].

5) Station scenario: Station scenario is an important part of HST railway. Generally, it consists of a platform nearby the track, a depot providing some tickets services and waiting room [5]. There are mainly three types of stations, i.e., small-size, medium and large-size stations. As to the small-size and medium stations, the LoS and NLoS components are existed which are similar to the rural area scenarios. As to the large ones, there are usually big awnings on the top of rails, which has a significant impact on the wireless signal propagation, especially at the moment of train moving into or out of stations [5], [8] with accelerated speed.

B. Cellular architecture of HST communication

As to the current Global System for Mobile Communication Railway (GSM-R) and the Long-Term Evolution-Railway (LTE-R) system which is based on the LTE-Advanced (LTE-A) system, both of them adopt the conventional network architecture in which HST users inside the train communicate with outdoor BSs directly [1]. This kind of architecture will result in high penetration losses, handover failure and high drop calls rate [2]. To mitigate the above problems, some new technologies have been proposed for future HST communication systems, such as MRS, DAS, and CoMP as shown in Fig. 1. Here, we will consider the MRS architecture in the adopted channel model.

III. HST Channel Statistical Properties in Different Scenarios

In this section, three of the most common HST scenarios are analyzed, i.e, rural area, viaduct, and cutting scenarios, which form around 80% of the HST scenarios along the Zhengzhou-Xian HST railway in China [12].

A. Non-Stationary Wideband MIMO Channel Model for HST Systems

Based on WINNER II and standard International Mobile Telecommunications-Advanced (IMT-A) systems which have adopted the promising MRS technology, a theoretical non-stationary GBSM for wideband MIMO HST channels has been proposed in [2]. To capture the non-stationarity of HST channels that has been widely reported in HST channel measurements, the proposed model introduced time-varying small-scale fading parameters, like angles of arrival (AoAs) and angles of departure (AoDs). However, the theoretical model assumes an infinite number of scatterers and hence cannot be used for simulations. Therefore, a corresponding simulation model with a finite number of effective scatterers was developed and the statistical properties of both models were derived [2]. By adopting some key scenarios-specific channel parameters, these models were further extended in [2] to be applicable on different HST scenarios, i.e., open-space, viaduct, and cutting scenarios. The genericness and accuracy of the proposed models have been verified in [1] using measurement data from the aforementioned scenarios. Here, we use the generic simulation model proposed in [1] for our analysis. The channel impulse response of the HST channel model between the pth transmitter and qth receiver can be expressed as

$$\begin{aligned}\tilde{h}_{pq}(t) &= \tilde{h}_{1,pq}(t) + \tilde{h}_{i,pq}(t) \\ &= \tilde{h}^{\mathrm{LOS}}_{1,pq}(t) + \tilde{h}^{\mathrm{SB}}_{1,pq}(t) + \sum_{i} h_{i,pq}(t) \end{aligned} \tag{1}$$

where

$$\tilde{h}^{\mathrm{LOS}}_{1,pq}(t) = \sqrt{\frac{K_{pq}(t)}{K_{pq}(t)+1}} e^{-j2\pi f_c \tau_{pq}(t)} e^{j2\pi f_{\max} t \cos\left(\tilde{\phi}^{\mathrm{LOS}}_{T_p}(t) - \gamma_R\right)} \tag{2}$$

$$\tilde{h}^{\mathrm{SB}}_{1,pq}(t) = \sqrt{\frac{\Omega_{1,pq}}{K_{pq}(t)+1}} \sum_{n_1=1}^{N_1} \frac{1}{\sqrt{N_1}} e^{j\left(\psi_{n_1} - 2\pi f_c \tau_{pq,n_1}(t)\right)} \times e^{j2\pi f_{\max} t \cos\left(\tilde{\phi}^{(n)}_{\mathrm{R}}(t) - \gamma_R\right)} \tag{3}$$

$$\tilde{h}_{i,pq}(t) = \sqrt{\Omega_{i,pq}} \sum_{n_i=1}^{N_i} \frac{1}{\sqrt{N_i}} \times e^{j\left(\psi_{n_i} - 2\pi f_c \tau_{pq,n_i}(t)\right)} \times e^{j2\pi f_{\max} t \cos\left(\tilde{\phi}^{(n_i)}_{R}(t) - \gamma_R\right)}, \quad 1 < i \leq I \tag{4}$$

It is worth mentioning that the parameters $K_{pq}(t)$, $\tau_{pq}(t)$, $\phi_{T_p}^{\mathrm{LOS}}(t)$, $\tau_{pq,n_i}(t)$, $\phi_R^{(n_i)}(t)$ in (2), (3), (4) are all time-variant in order to describe the non-stationarity of HST channels. The $\tau_{pq}(t)$ is related to the distance $D_s(t)$ between transmitter and receiver, $\tau_{pq,n_i}(t)$ can be obtained from the distance $\xi_{\mathrm{T}}^{(n_i)}(t)$ between transmitter and effective scatterer and distance $\xi_{\mathrm{R}}^{(n_i)}(t)$ between effective scatterer and receiver. ψ_{n_i} designates the initial angular values with uniform distribution, and γ_R denotes the angle of MRS motion. The time varying and multipath characteristics can be described by the ellipse model illustrated in Fig. 2.

B. Channel statistical properties in different HST scenarios

In this section, based on the non-stationary HST simulation channel model, the channel statistical properties in different scenarios are presented with the assumptions of uncorrelated scatterers and antenna stationarity [2]. Here, we mainly focus on the first tap of the channel, which consists of the LoS and single-bounced (SB) components, to carry out our derivations.

1) Time-Variant Space CCF: The stationary properties of wideband MIMO HST channel can be presented by the correlation properties of two arbitrary channel impulse responses, $\tilde{h}_{i,pq}(t)$ and $\tilde{h}_{i,p'q'}(t)$ in different time intervals and different antenna elements. The time-variant space-time (ST) correlation function (CF) can be derived as

$$\begin{aligned}\tilde{R}_h(t,\Delta x_T,\Delta x_R,\Delta t) &= \frac{E\{\tilde{h}_{i,pq}(t)\tilde{h}_{i,p'q'}(t-\Delta t)\}}{\sqrt{\Omega_{i,pq}\Omega_{i,p'q'}}} \\ &= \tilde{R}_h^{LOS}(t,\Delta x_T,\Delta x_R,\Delta t)+\tilde{R}_h^{SB_i}(t,\Delta x_T,\Delta x_R,\Delta t)\end{aligned} \tag{5}$$

By imposing $\Delta t = 0$ in (5), we can get the time-variant space CCF between two arbitrary channel impulse responses, which can be expressed as

$$\begin{aligned}\tilde{\rho}(t,\Delta x_T,\Delta x_R) &= \frac{E\left\{\tilde{h}_{i,pq}(t)\,\tilde{h}_{i,p'q'}^{*}(t)\right\}}{\sqrt{\Omega_{i,pq}\Omega_{i,p'q'}}} \\ &= \tilde{R}_h(t,\Delta x_T,\Delta x_R,0)\end{aligned} \tag{6}$$

2) Time-Variant ACF: Based on the ST CF, the time-variant ACF can be obtained by imposing $\Delta x_T = 0$ and $\Delta x_R = 0$, which can be expressed as

$$\tilde{r}(t,\Delta t) = \frac{E\left\{\tilde{h}_{i,pq}(t)\,\tilde{h}_{i,pq}^{*}(t-\Delta t)\right\}}{\sqrt{\Omega_{i,pq}\Omega_{i,p'q'}}} = \tilde{R}_h(t,0,0,\Delta t) \tag{7}$$

Using the ACF, the delay spread of propagation channel can be calculated. Both the time-variant CCF and ACF are related to the Ricean K-factor, $K_{pq}(t)$, which can be used to reflect the proportion of LoS component and the distribution of scatterers in different HST scenarios.

3) Time-variant SD PSD: The time-variant SD PSD is also one of the important channel characteristics, which can reflect the PSD distribution along the Doppler frequency of signals. Generally, it can be obtained by applying the Fourier transformation on the time-variant ST CF in terms of Δt. The derivations can be expressed as

$$W(t,f,\Delta x_T,\Delta x_R) = \int \tilde{R}_h(t,\Delta x_T,\Delta x_R,\Delta t)e^{-j2\pi f\Delta t}d\Delta t \tag{8}$$

TABLE I
PARAMETERS OF SIMULATIONS IN DIFFERENT SCENARIOS.

Parameters	Rural area	Viaduct	Cutting
LoS Ricean Factor (dB)	6 [1]	3.66 [7]	1.88 [6]
Distance between MRS and BS (m)	1000	819	1200
Effective number N	50	60	70
Speed of MRS (km/h)	360	360	360
Maximum Doppler shift (Hz)	1330	1330	1330
Carrier frequency (GHz)	4	4	4

IV. The simulation and analysis of channel statistical properties in different HST scenarios

In this section, the channel statistical properties of the proposed simulation model in different HST scenarios, i.e., the rural area, cutting, and viaduct scenarios, are analyzed and compared. HST channel parameters have different values in different scenarios, e.g., the value of Ricean K-factor, which have an important impact on the evaluation of the channel characteristics. The parameters for our simulation and analysis are listed on Table I.

A. Time-variant space CCF

Based on the HST simulation channel model [2], the absolute values of the time-variant space CCF of the first and second taps of the non-stationary MIMO channel model in different HST scenarios are illustrated in Fig. 3 and Fig. 4, respectively. Using (2), (3) and (6), a comparison of time-variant space CCF of the first tap which consists of LoS and SB components is shown in Fig. 3. From Table I, we can see that the value of the Ricean K-factor in rural area scenario is the largest one, followed by the viaduct's and then the cutting's. Since the Ricean K-factor describes the proportion of LoS component on SB components, the rural area scenario seem to have the strongest LoS component. Fig. 3 shows that highest correlation values are encountered in rural area, then in viaduct scenario, and finally in cutting scenario. Fig. 4 shows the number of effective scatterers of the second tap that are needed to match theoretical model very well in different HST scenarios. From this figure, we can see that there are more effective scatterers in cutting scenario, in which $N = 70$.

B. Time-variant ACF

By using the (2), (3) and (7), and substituting the parameters in Table I, Fig. 5 shows the comparison of absolute values of time-variant ACF of first tap. From this figure, we can see a highest correlation in rural area scenario, compared with the viaduct and cutting scenarios. It also shows us that different scenarios have different correlation, which is related to the value of the Ricean K-factor [1]. Fig. 6 shows the number of effective scatterers of the second tap of the ACF, in which they

can fit the theoretical model very well in different scenarios. From this figure, we can see that there are more effective scatterers in cutting scenarios, that is $N = 70$, then is $N = 60$ in viaduct, finally is $N = 50$ in rural area. All of above show that it will bring more effect scatterers in cutting scenarios than others.

C. Time-variant SD PSD

Fig. 7 compares the time-variant SD PSDs of the simulation model at same time $t = 0$ for isotropic assumption. From this figure, we can easily notice that the SD PSDs are presented as U-shaped in different scenarios, which can be obtained by ACF applying the Fourier transform from time interval Δt to Doppler frequency f. It can be observed from Fig. 7 that there is the lowest power in zero Doppler frequency, then increase gradually in non-zero Doppler frequencies. PSDs in different scenarios have the same variation trends.

V. Conclusions

In this paper, based on a verified wideband generic non-stationary HST channel model, some channel statistical properties such as the ACF, space CCF, and PSD in three different HST scenarios (i.e., rural area, viaduct, and cutting scenarios) have been investigated and compared. It has been shown that the Ricean K-factor has a significant impact on the ACF and space CCF of the channel model in different HST scenarios. Moreover, the scattering richness degree of the HST scenario, represented by the number of effective scatterers, can vary among the studied HST scenarios.

Acknowledgment

The authors gratefully acknowledge the support of this work from the EU H2020 5G Wireless project (No. 641985), EU FP7 QUICK project (No. PIRSES-GA-2013-612652), 863 Project in 5G (No. 2014AA01A707), National Science and Technology Major Project (No. 2014ZX03003012-001), and National Natural Science Foundation of China through the Major International Joint Research Project (No. 61210002).

References

[1] A. Ghazal, C.-X Wang, Y. Liu, P.-Z. Fan, M. K. Chahine, "A generic non-stationary MIMO channel model for different high-speed train scenarios," in *IEEE Proc. ICCC'15*, Shenzhen, China, Nov. 2015, pp. 885–897.

[2] A. Ghazal, C.-X. Wang, B. Ai, D. Yuan, and H. Haas, "A non-stationary wideband MIMO channel model for high-mobility intelligent transportation systems," *IEEE Trans. Intell. Transp. Syst.*, vol. 16, no. 2, pp. 885-897, Apr. 2015.

[3] C.-X. Wang, F. Haider, X. Gao, X.-H. You, Y. Yang, D. Yuan, H. Aggoune, H. Haas,S. Fletcher, E. Hepsaydir, "Cellular architecture and key technologies for 5G wireless communication networks," *IEEE Commun. Mag.*, vol. 52, no. 2, pp. 122-130, Feb. 2014.

[4] D. Lee, H. Seo, B. Clerckx, E. Hardouin, D. Mazzarese, S. Nagata, and K. Sayana, "Coordinated multipoint transmission and reception in LTE-advanced: deployment scenarios and operational challenges," *IEEE Commun. Mag.*, vol. 50, no. 2, pp. 148-155, Feb. 2012.

[5] B. Ai, R. He, Z. Zhong, K. Guan, B. Chen, P. Liu, and Y. Li, "Radio wave propagation scene partitioning for high-speed rails," *Int. J. Antennas Propag.*, vol. 2012, Article ID 815232, 7 pages, 2012. doi 10.1155/2012/815232.

[6] R. He, Z. Zhong, B. Ai, J. Ding, Y. Yang, and A. F. Molisch, "Short-term fading behavior in high-speed railway cutting scenario: measurements, analysis, and statistical models," *IEEE Trans. Antennas Propag.*, vol. 61, no. 4, pp. 2209-2222, Apr. 2013.

[7] R. He, Z. Zhong, B. Ai, and J. Ding, "Measurements and analysis of short-term fading behavior for high-speed rail viaduct scenario," in *IEEE Proc. ICC'12*, Ottawa, Canada, June 2012, pp. 4563–4567.

[8] K. Guan, Z. Zhong, B. Ai, and T. Kurner, "Propagation measurements and analysis for train stations of high-speed railway at 930 MHz," *IEEE Trans. Veh. Technol.*, vol. 63, no. 8, pp. 3349-3516, Oct. 2014.

[9] C.-X. Wang, A. Ghazal, B. Ai, Y. Liu, and P. Fan, "Channel measurements and models for high-speed train communication systems: a survey," *IEEE Commun. Surveys Tuts*, accepted for publication.

[10] Y. Liu, C.-X. Wang, A. Ghazal, S. Wu, and W. Zhang, "A multimode waveguide tunnel channel model for high-speed train wireless communication systems," in *Proc. EuCAP'15*, Lisbon, Portugal, Apr. 2015, pp. 1–5.

[11] C. Briso-Rodriguez, J. M. Cruz, and J. I. Alonso, "Measurements and modeling of distributed antenna systems in railway tunnels," *IEEE Trans. Veh. Technol.*, vol. 56, no. 5, pp. 2870-2879, Sept. 2007.

[12] R. He, Z. Zhong, B. Ai, and K. Guan, "Reducing the cost of high-speed railway communications: From the propagation channel view," *IEEE Trans. Intell. Transp. Syst.*, vol. 16, no. 4, pp. 2050–2060, Aug. 2015.

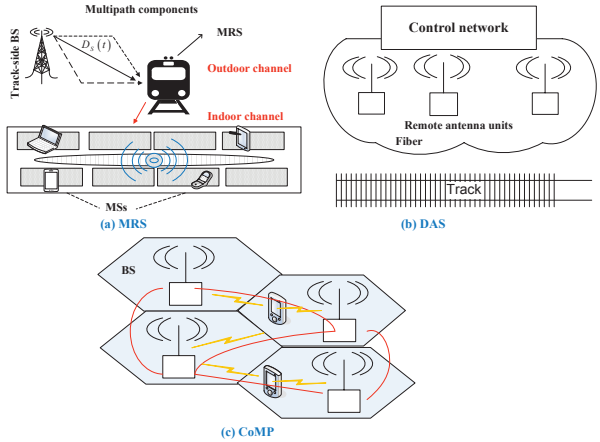

Fig. 1. Cellular architectures for HST communication systems.

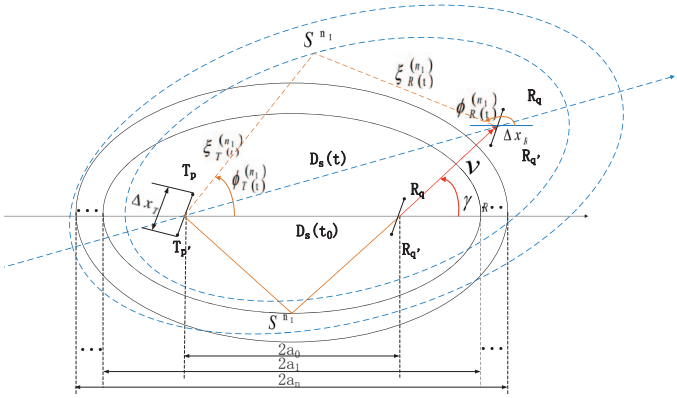

Fig. 2. A HST MIMO channel model with multiple con-focal ellipses considering time-variant characteristics.

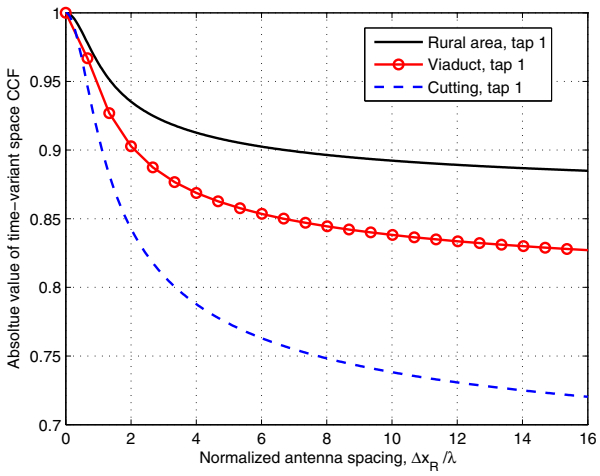

Fig. 3. Comparison of the time-variant space CCFs of the first tap in different HST scenarios.

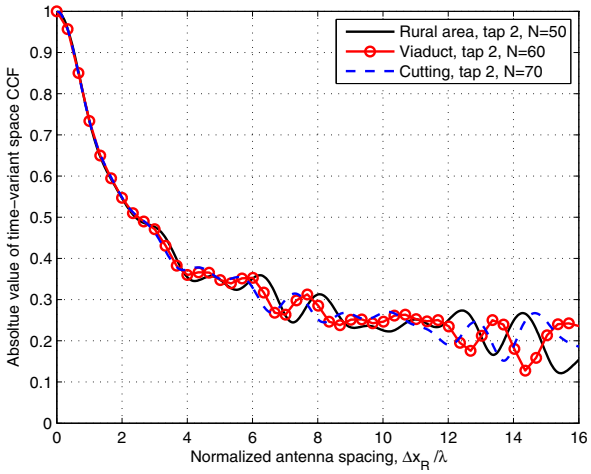

Fig. 4. Comparison of the time-variant space CCFs of the second tap of the simulation model in different HST scenarios.

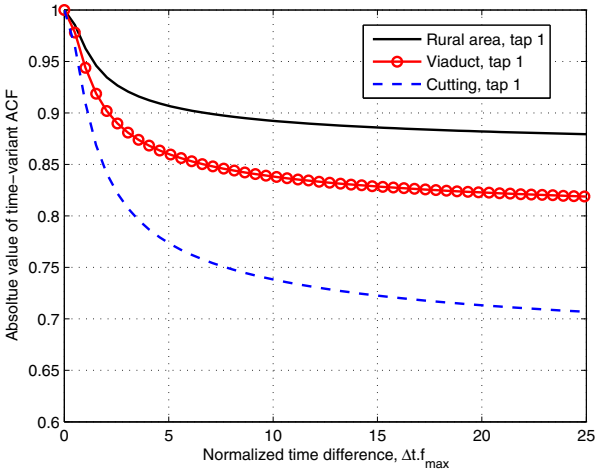

Fig. 5. Comparison of the time-variant ACFs of the first tap in different HST scenarios.

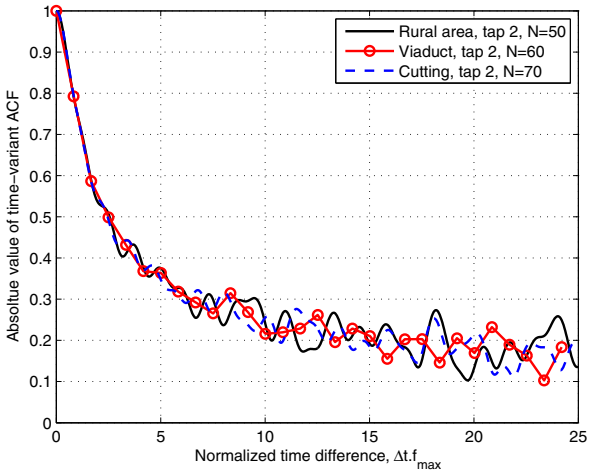

Fig. 6. Comparison of the time-variant ACFs of the second tap of the simulation model in different HST scenarios.

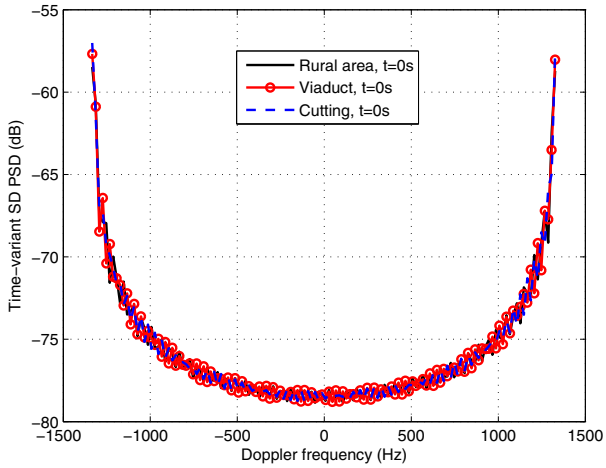

Fig. 7. Comparison of the SD PSDs of the simulation model in different HST scenarios for the isotropic case.